Chemical Science

Accepted Manuscript

This article can be cited before page numbers have been issued, to do this please use: G. Liang, D. Chen, Z. Long, H. Zhuo, X. Zhong, X. Chen, H. Shao, Z. Mo and X. Chen, *Chem. Sci.*, 2025, DOI: 10.1039/D5SC05093F.

ROYAL SOCIETY OF CHEMISTRY

rsc.li/chemical-science

ARTICLE

View Article Online
DOI: 10.1039/D5SC05093F

Efficient Capture of Trace Benzene Vapor by Metal-Organic Frameworks Modified with Macrocyclic Pyridyl Ligands

Received 00th January 20xx,
Accepted 00th January 20xx

DOI: 10.1039/x0xx00000x

Gang Liang, [a] De-Jian Chen, [a] Zhu-Jun Long, [a] Hao Zhuo, [b] Xiao-Feng Zhong, [b] Xiong-Hai Chen, [b] Huai-Yu Shao, [c] Zong-Wen Mo, *[ad] and Xiao-Ming Chen [b]

The capture of trace benzene vapor is an important and huge challenge due to serious toxicity. Physisorbents usually exhibit weak interactions especially in the presence of trace concentrations, thus possessing poor removal performance. Herein, an efficient post-synthetic modification strategy with various mono-, bi-, and tri-pyridyl derivative ligands was performed on the parent [$Fe_3(\mu_3$-O)(OH)$(H_2O)_2$(pet)] (**NU-1500(Fe)**, H_6pet = peripherally extended triptycene, 4,4',4'',4''',4'''',4'''''-(9,10-dihydro-9,10-[1,2]benzenoanthracene-2,3,6,7,14,15-hexayl)hexabenzoic acid) with large hexagonal pores (14 × 19 Å^2) and modifiable metal sites. Remarkably these MOFs can regulate the performance of trace adsorption of benzene. Among them, the tri-pyridyl ligand modified [$Fe_3(\mu_3$-O)(pet)(tph)] (**WYU-107**, Htph = 2,5,8-tri-(4-pyridyl)-1,3,4,6,7,9-hexaazaphenalene) reaches an uptake of 6.21 mmol/g at 298 K and P/P_0 = 0.01 by virtue of the significant interactions between the pore partitioned host-framework and benzene molecules, which shows a capture performance exceeding most of the reported porous materials. At the same time, breakthrough experiments revealed that **WYU-107** can capture trace benzene in the air, and *in situ* variable-pressure PXRD indicates the reversible deformation behavior during the adsorption process. Theoretical calculations and *in situ* single-crystal structure reveal that the significant interactions are closely related to the insertion of functional tph ligand, facilitating the capture of benzene vapor at trace level.

Introduction

According to the World Health Organization, benzene is a highly toxic carcinogen, which seriously endangers human health even at trace levels.[1] Therefore, it is necessary to develop functional materials to realize efficient benzene vapor capture, especially at trace concentrations. Current methods to remove benzene vapor from indoor air include oxidation and adsorption by functional porous materials. However, high energy consumption and low adsorption efficiency (weak interactions between the host-framework and benzene molecules) limit the application.[2-6]

As a booming sort of porous material, metal-organic frameworks (MOFs) are well-known for their highly designable, tunable structures and pore surfaces, which play important roles in numerous applications,[7-8] such as gas storage/capture,[9] selective separation and molecular sensing.[10-12] Recently, a few MOFs have demonstrated huge potential in the removal of saturation benzene vapor even at trace levels. For example, the unique double-walled MOF, [Co(dpn)] (BUT-54(Co), H_2dpn = 2,7-di(1*H*-pyrazol-4-yl)naphthalene) achieved a benzene vapor uptake of 4.31 mmol/g at P/P_0 = 0.01 due to the multiple C–H···π interactions between dpn^{2-} ligands and benzene molecules.[11] Similarly, the benzene vapor uptake of [Al(μ-O)$_2$(μ-OH)(dbp)] (ZJU-520(Al), H_2dbp = 4,6-di(4-carboxyphenyl)pyrimidine) reaches 5.98 mmol/g at 298 K and P/P_0 = 0.01 based on the strong Al···π interactions between AlO_6 clusters and benzene molecules.[13] Besides, single-atom(Zn) sites in defected-MIL-125, [$Ti_8O_8(\mu$-OH)$_4$(bdc)$_6$] (H_2bdc = 1,4-benzenedicarboxylic acid), can serve as potential sites toward benzene molecules, achieving the record high benzene uptake (7.63 mmol/g) at 298 K and 1.2 mbar.[14] These results clearly demonstrate that enhancing the interaction between host-framework and benzene molecules is the key to achieving efficient capture of benzene vapor.[15-16] Despite the progress in trace adsorption of benzene vapor, the efficient capture based on directional assembly remains a huge challenge. In principle, the introduction of aromatic macrocyclic groups into MOF frameworks is an effective approach to improve the adsorption of benzene vapor by virtue of the strong interaction between aromatic macrocyclic ligand and benzene molecules. For example, [Sr_2(bindi)(DMF)(H_2O)] (**WYU-61**, H_4bindi = *N*,*N*′-bis(5-isophthalic acid)naphthalenediimide, DMF = *N*,*N*-dimethylformamide), a MOF with aromatic macrocyclic bindi ligands, exhibits the unique "bilateral π-π stacking" host-guest interaction between benzene molecules and the macrocyclic ligands, realizing the adsorption and detection of trace benzene vapor.[17] However, poor solubility of macrocyclic derivative ligands and unpredictability of the direct synthetic method, as well as low porosity of host-frameworks lead to the difficulty in orientated construction of MOFs. In contrast, the insertion of aromatic macrocyclic ligands into the parent MOFs by post-synthetic modification (PSM) is an effective strategy, and the key is the compatibility of the parent MOFs and inserted ligands.[18-21]

Here, we report a series of MOFs (**WYU-100~108**, WYU = Wuyi University), synthesized by PSM of [$Fe_3(\mu_3$-O)(OH)$(H_2O)_2$(pet)] **(NU-1500(Fe)**,[22] H_6pet = peripherally extended triptycene, 4,4',4'',4''',4'''',4'''''-(9,10-dihydro-9,10-

[a] School of Environmental and Chemical Engineering, Wuyi University, Jiangmen, Guangdong 529020, China
[b] MOE Key Laboratory of Bioinorganic and Synthetic Chemistry, GBRCE for Functional Molecular Engineering, School of Chemistry, IGCME, Sun Yat-Sen University, Guangzhou 510275, China
[c] Joint Key Laboratory of the Ministry of Education, Institute of Applied Physics and Materials Engineering, University of Macau, Macau SAR, China
[d] Guangdong Provincial Laboratory and Fine Chemical Engineering Jie Yang Center
†Electronic Supplementary Information (ESI) available. See DOI: 10.1039/x0xx00000x

View Article Online
DOI: 10.1039/D5SC05093F

[1,2]benzenoanthracene-2,3,6,7,14,15-hexayl)hexabenzoic acid) with large hexagonal pores (14 × 19 Å^2) and various modifiable metal sites for insertion of various pyridyl ligands (Figure 1a).

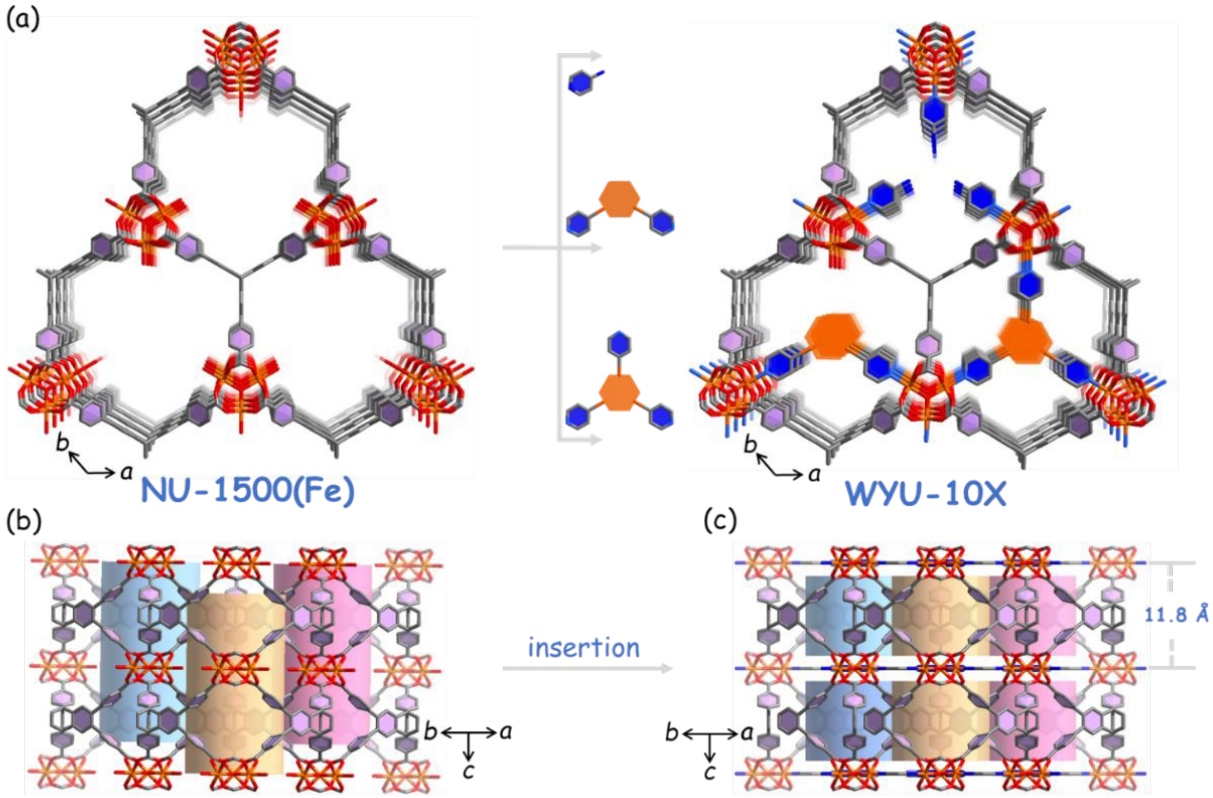

Figure 1. (a) The post-modification strategy of various pyridyl derivative ligands based on the prototype **NU-1500(Fe)**. The comparison of pore void between (b) **NU-1500(Fe)** and (c) post-modification **WYU-107**.

Interestingly, the insertion is not only feasible for smaller mono-pyridyl derivative ligands, but also for bi-pyridyl derivative ligands, and even for larger tri-pyridyl derivative ligands, compared with the limited porosity MOFs, such as [$Zr_6(\mu_3$-O)$_4(\mu_3$-OH)$_4$(OH)$_4$(H_2O)$_4$(ettc)$_2$] (WSU-5, H_4ettc = 4',4''',4'''''',4''''''''-(ethene-1,1,2,2-tetrayl)tetrakis([1,1'-biphenyl]-4-carboxylic acid)) and [$Zr_6(\mu_3$-O)$_4(\mu_3$-OH)$_4$(HCOO)$_4$(tcpe)$_2$ (H_4tcpe = 1,1,2,2-tetra(4-carboxylphenyl)ethylene).[23-24] The saturation uptake of benzene vapor, stepped pressure, and the trace adsorption can be regulated by the insertion of different types of pyridyl derivative ligands based on the various host-guest interaction. Notably, [$Fe_3(\mu_3$-O)(pet)(tph)] (**WYU-107**) containing the tri-pyridyl derivative ligand 2,5,8-tri-(4-pyridyl)-1,3,4,6,7,9-hexaazaphenalene (Htph) achieves an exceptional benzene uptake of 6.21 mmol/g by virtue of the strong interactions between the larger conjugated hexaazaphenalene-based ligand and benzene molecules at P/P_0 = 0.01, which is three times that of the parent **NU-1500(Fe)** (2.12 mmol/g).[25] As far as we know, **WYU-107** is the first post-synthetic modified MOF showing highly efficient capture of benzene vapor at trace level, being superior to most of the reported porous materials, and only next to the defected-MIL-125-X (X = Mn, Co, Ni, Cu, Zn). Furthermore, breakthrough experiments further demonstrate that **WYU-107** has excellent potential for trace benzene capture. The combination of *in situ* single-crystal X-ray diffraction (SCXRD) and theoretical calculations demonstrates that the large aromatic tph ligand is conducive to the benzene vapor adsorption under low pressure.

Results and Discussion

NU-1500(Fe) with **acs** topology is constructed from pet ligands and trinuclear [$Fe_3(\mu_3$-O)(H_2O)$_2$(OH)(RCOO)$_6$] clusters. There are large hexagonal channels (14 × 19 Å^2) in the framework along the *c*-axis, and the pore ratio reaches 74.8%. More importantly, there are two terminal H_2O and one OH^- ligands in the cluster, which can serve as perfect sites for ligand replacement by PSM. On the other hand, the compatibility of the substituting ligand and the spatial arrangement of the modifiable sites are also significant factors. Compared to **NU-1500(Fe)**, other parent MOFs, such as [Co_2(dobdc)] (MOF-74(Co), H_4dobdc = 2,5-dihydroxyl-1,4-benzenedicarboxylic acid,[26] [$Fe_3(\mu_3$-O)(tba)$_3$(OH)(H_2O)$_2$] (MIL-88A(Fe), H_2tba = *trans*-2-butenedioic acid) and [$Zr_{12}(\mu$-O)$_8(\mu$-OH)$_8$(CH_3COO)$_{12}$(tcpb-Br_2)$_3$] (NU-600, H_4tcpb-Br_2 = 4-dibromo-2,3,5,6-tetrakis(4-carboxyphenyl)benzene) exhibit more restricted pore sizes and modifiable sites. There inherent limitation hinder to accommodate the extended or bulky organic ligands.[27-28] As far as we know, few MOFs can achieve various types of ligand

View Article Online
DOI: 10.1039/D5SC05037F

insertion, not to mention to the macrocyclic ligands with large molecular sizes. Fortunately, the combination of large pore size and three modifiable sites in the parent **NU-1500(Fe)** allows for the modifications of not only smaller mono-pyridyl derivative ligands, but also larger bi-pyridyl and even tri-pyridyl derivative ligands (Figure S1). In principle, the insertion is feasible as long as the ligand length of L_1 (mono-pyridyl ligand) is shorter than the pore size, or the shapes and sizes of L_2 (bi-pyridyl ligand) and L_3 (tri-pyridyl ligand) are adaptable to two and three modifiable sites, respectively (Figure S2).

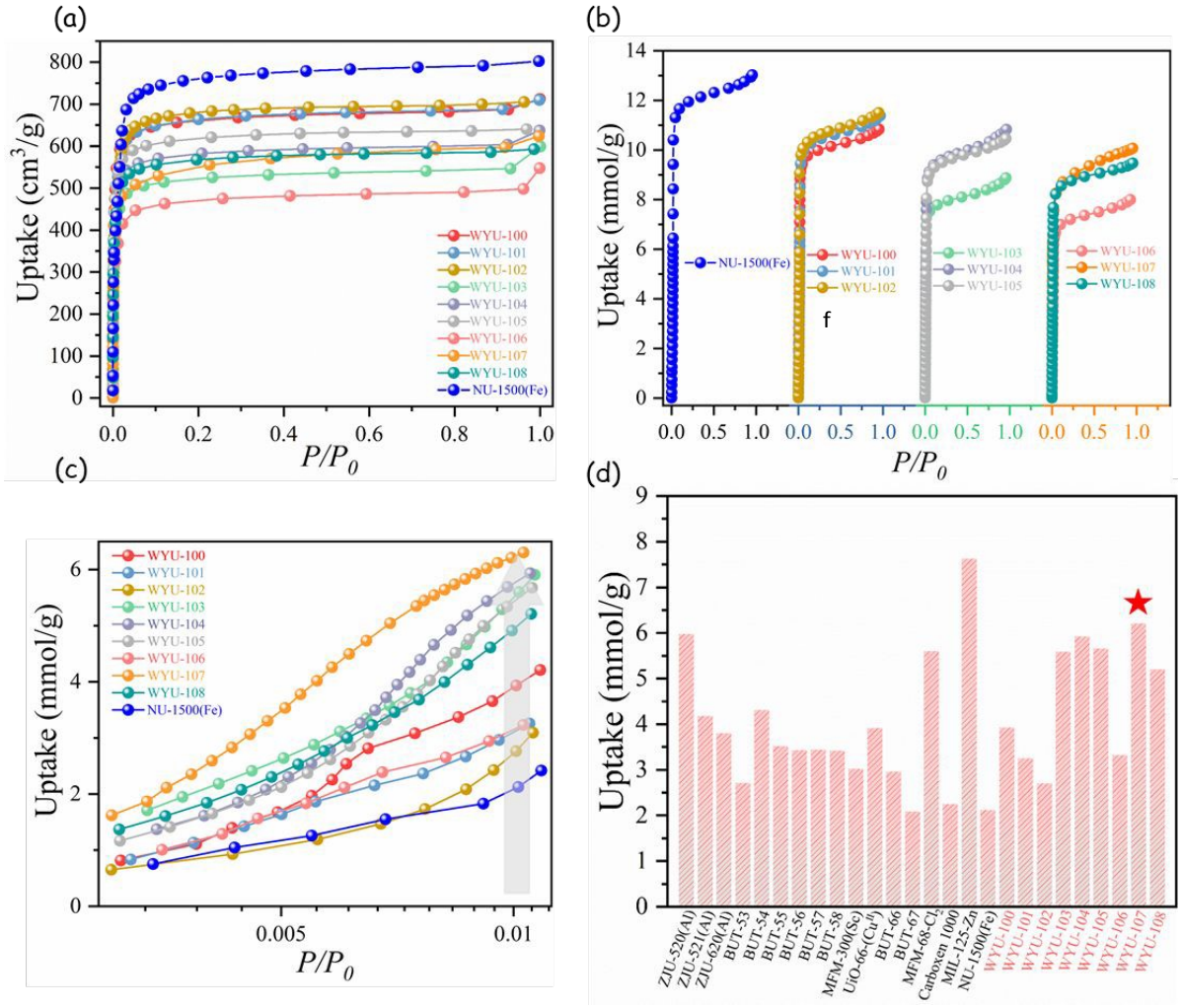

Figure 2. (a) N_2 sorption isotherms at 77 K and (b) benzene vapor adsorption isotherms at 298 K for **WYU-100~108** and **NU-1500(Fe)**. (c) Logarithmic-scale plots of P/P_0 = 0.01 to view the adsorption of benzene at low partial pressures. (d) The performance comparison of trace benzene vapor uptakes for various MOFs at P/P_0 = 0.01.

The PSM strategy was proved by single-crystal X-ray diffraction (SCXRD) (Tables S2-S5), as well as ^{1}H NMR spectra. The ratio of H_6pet:L_1 (apy, ina, pyb) is close to 1:3 (Figures S3-S5), suggesting that three terminal H_2O/OH^- ligands in a [$Fe_3(\mu_3$-O)$(H_2O)_2$(OH)$(RCOO)_6$] cluster can be replaced by mono-pyridyl ligands to give the corresponding modified [$Fe_3(\mu_3$-O)$(apy)_3$(pet)]·*x* (**WYU-100**, apy = 4-aminopyridine, *x* = counter anions), which crystallizes in the hexagonal *P6m2* space group. There are three apy ligands inserted into each trinuclear cluster of the parent **NU-1500(Fe)** since the length of the ligand (4.6 Å) is less than d_1 (Figure S2). Furthermore, similar mono-pyridyl ligands (ina = isonicotinic acid, pyb = pyridine-4-boronic acid) can also be used to modify **NU-1500(Fe)** into [$Fe_3(\mu_3$-O)$(ina)_3$(pet)]·*x* (**WYU-101**) and [$Fe_3(\mu_3$-O)$(pyb)_3$(pet)]·*x* **(WYU-102)**, respectively. However, the orientations of apy and ina ligands in the frameworks of **WYU-100** and **WYU-101** are vertical, while that of pyb ligand in **WYU-102** is parallel, to the trinuclear core (Figure S12).

Considering the distribution of trinuclear clusters in the hexagonal pore, bi-pyridyl ligands with a length close to 12.6 Å (the distance between two Fe^{3+} ions in adjacent trinuclear clusters, Figure S2) can also modify **NU-1500(Fe)**. The larger N^1,N^3-di(pyridine-4-yl)isophthalamide (bpipa) ligand with functional amide groups was then inserted into it to furnish a new MOF, [$Fe_3(\mu_3$-O)(OH)(pet)(bpipa)] (**WYU-103**). The ratio of H_6pet:L_2 (L_2 = bpipa, dpyc, or dpyn) is close to 1:1 based on ^{1}H NMR spectra measurements (Figures S6-S8), suggesting that two terminal H_2O molecules in each trinuclear cluster can be replaced by pyridyl derivative ligands, transforming the 6-connected **NU-1500(Fe)** into the 8-connected **WYU-103**. Consequently, the hexagonal channel is partitioned into two smaller ones.[15] Similarly, other bi-pyridyl ligands featuring,

View Article Online DOI: 10.1039/D5SC05097F

larger bending angles (103.5°) and longer lengths (11.95 Å), such as 3,6-di(pyridin-4-yl)-9*H*-carbazole (dpyc) and 2,7-di(4-pyridyl)naphtalene (dpyn), can also facilitate the assembly of similar 8-connected [Fe_3(μ_3-O)(OH)(pet)(dpyc)] (**WYU-104**), [Fe_3(μ_3-O)(OH)(pet)(dpyn)] (**WYU-105**). These result further demonstrate the high adaptability of **NU-1500(Fe)** to diverse ligand modifications.

Based on the above results, PSMs with larger tri-pyridyl derivative ligands (tpybtc = *N*,*N*′,*N*″-tris(4-pyridinyl)-1,3,5-benzenetricarboxamide, Htph = (2,5,8-tri-(4-pyridyl)-1,3,4,6,7,9-hexaazaphenalene, tpvb = 1,3,5-tris((*E*)-2-(pyridin-4-yl)vinyl)benzene) were further performed to verify the feasibility of this strategy.[29] SCXRD reveals that three terminal H_2O/OH^- ligands on the trinuclear cluster can be completely replaced by the tri-pyridyl ligands to achieve 9-connected MOFs, [Fe_3(μ_3-O)(pet)(tpybtc)]·*x* **(WYU-106)**, [Fe_3(μ_3-O)(pet)(tph)] **(WYU-107)** and [Fe_3(μ_3-O)(pet)(tpvb)]·*x* **(WYU-108)**. ^{1}H NMR spectral measurements further verified that the ratio of H_6pet:L_3 (L_3 = tpybtc, tph, tpvb) is close to 1:1 (Figures S9-S11). The replaced groups in the ligands derived from **WYU-106~108** were further confirmed by FT-IR spectra (Figure S15). As the terminal OH^- ligand is replaced by deprotonated tph ligand, **WYU-107** becomes a neutral framework. In contrast, there are counter anions accommodated in **WYU-106** and **WYU-108**, although these anions cannot be clearly determined by SCXRD due to their serious disorder. Interestingly, the symmetries of **WYU-106~108** are maintained after the ligand insertion of tpybtc, Htph and tpvb due to the geometric compatibility of the ligands and the rigidity of the parent framework. It is worth noting that the large 3D pore in **NU-1500(Fe)** is partitioned into three smaller ones after the above modification. Notably, the porosity decreased from 74.8% of **NU-1500(Fe)** to 69% of **WYU-100~102** with mono-pyridyl ligands, to 67% of **WYU-103~105** with bi-pyridyl ligands, and finally to 66% of **WYU-106~108** with tri-pyridyl ligands. More importantly, the functional N and O sites are successfully introduced into the host-framework upon modification. For example, the anionic tph ligand contains a large hexaazaphenalene moiety with six nitrogen atoms, which is conducive to the formation of multiple hydrogen bonds between the macrocycle moiety and guest molecules. In other words, various types of pyridyl ligands can be inserted into the host-framework to regulate the functionality.

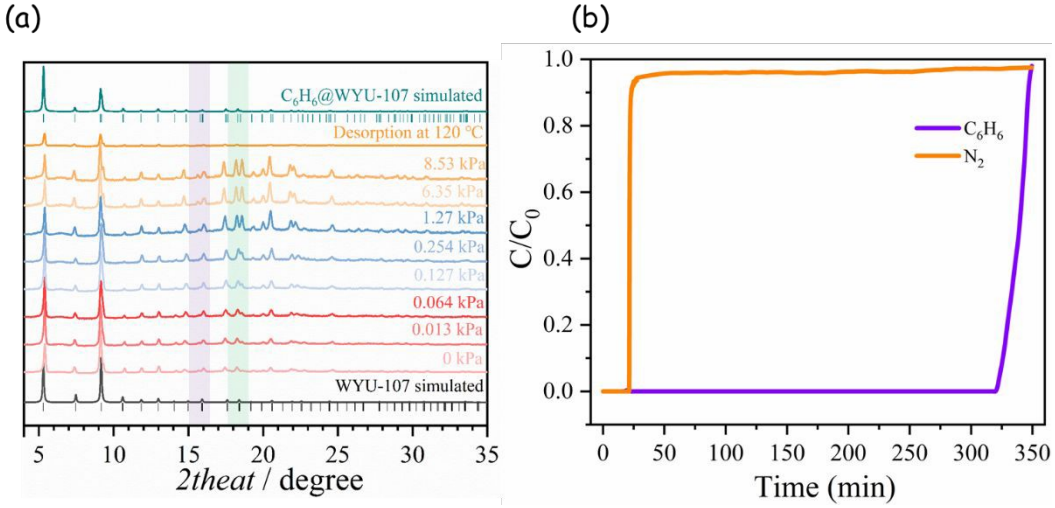

Figure 3. (a) *In situ* variable-pressure PXRD patterns of **WYU-107**, which collected under benzene vapor pressure from 0 to 8.53 kPa (guest-free to **C_6H_6@WYU-107**) and desorption at 120 ℃ after adsorption process. (b) Benzene breakthrough curves for **WYU-107** in air at 298 K.

The purities of as-synthesized **NU-1500(Fe)** and **WYU-100~108** were checked by powder X-ray diffraction (PXRD) patterns, which are consistent with the simulated ones, indicating the high purity and crystallinity (Figures S13-S14). TG curves of as-synthesized **WYU-100~108** showed large weight loss from room temperature to 350 °C due to the removal of free guest and coordination solvent molecules within the pore, and the remaining host framework decomposed above 400 °C (Figures S16-S17). The porosities of **WYU-100~108** were measured by N_2 sorption isotherms at 77 K, which showed typical type-I curves (Figure 2a). The adsorption capacities of these frameworks are lower than the parent **NU-1500(Fe)** attributed to the insertion of various ligands. Specifically, the pore volumes of **NU-1500(Fe), WYU-100**, **WYU-105** and **WYU-107** can be calculated to be 1.25, 1.07, 0.99 and 0.93 $cm^3\ g^{-1}$, respectively, which are close to their theoretical values (1.40, 1.19, 1.13 and 0.97 $cm^3\ g^{-1}$). Fitting the adsorption isotherms of **NU-1500(Fe) WYU-100**, **WYU-105** and **WYU-107** by the Brunauer-Emmett-Teller (BET) model gave the surface areas of 2900, 2690, 2480 and 2070 $m^2\ g^{-1}$, respectively. As expected, the insertion of different sized ligands (L_1 to L_3) can regulate the pore size of the host-framework.

Nonlocal Density Functional Theory (NLDFT) calculations gave broad pore size distributions centered range from 8.3 to 12 Å (Figure S18), which is smaller than parent **NU-1500(Fe)** (14 Å) due to the various pyridyl ligand insertion. Interestingly, the pore window of **WYU-107** was partitioned into three triangular channels (7.8 × 6.9 $Å^2$), being consistent with the value from the pore size distribution. This pore size compatibility with molecules significantly promotes the host-guest interaction, which is conducive to improving the capture performance. In addition, these MOFs retain their frameworks after being exposed to air or immersed in aqueous solutions in a wide pH range from 3 to 10 for one year (Figures S19-S21). Moreover, ^{1}H

View Article Online
DOI: 10.1039/D5SC05975E

NMR measurement of **WYU-100~108** after post-treatment (the desorption MOFs was exposed to air for one year, and washed with DMF and acetone for several times) further verified the stability of inserted pyridyl ligand (Figures S3-S11). However, 77 K N_2 adsorption measurements of **WYU-100~108** after being exposed to the air one year were revealed a decline in saturated uptake. Among them, the uptake of tri-pyridyl modified MOFs (**WYU-107** and **WYU-108**) displayed a marginally smaller decline than those bi-pyridyl and mono-pyridyl modified MOFs (Figure S22). This trend was further corroborated by the result obtained from **WYU-107** after immersion at pH = 3 and pH = 10. These observations can be contributed to the higher structural connectivity, which is more conducive to the stability of the framework (Figure S23).

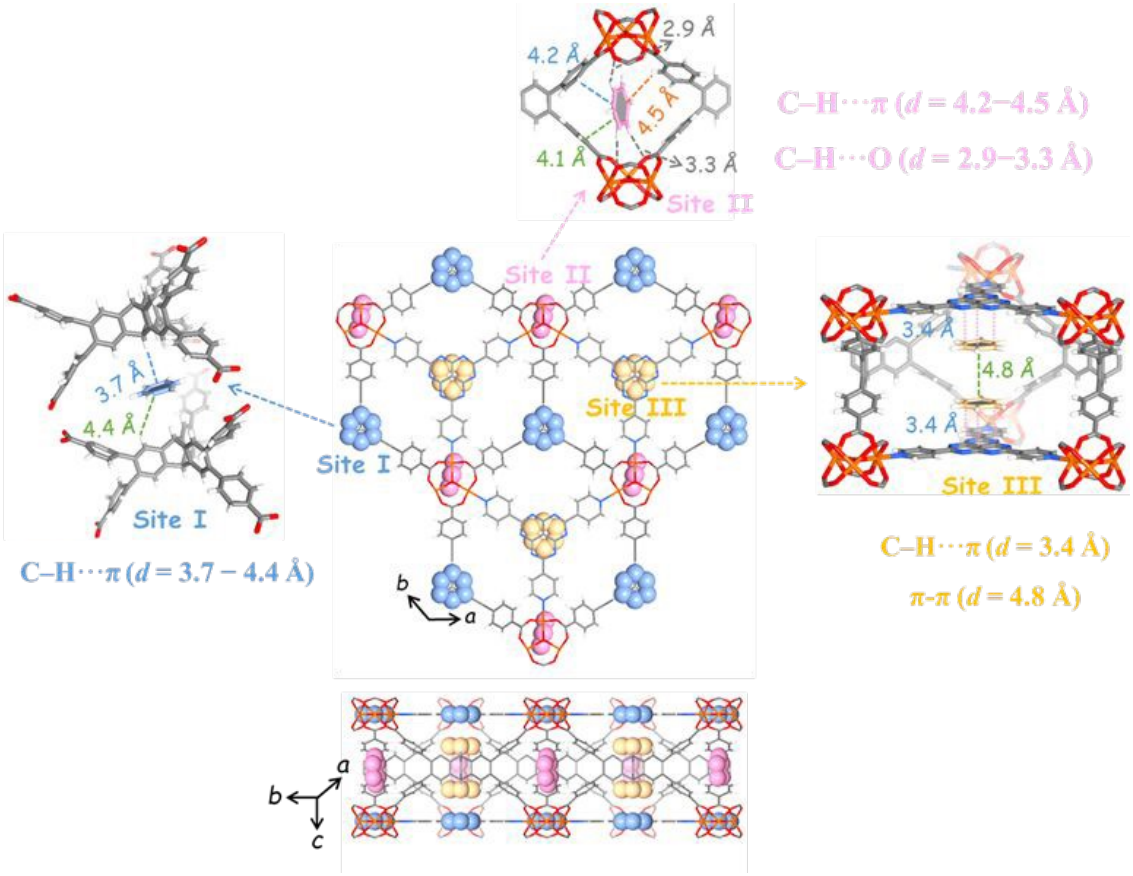

Figure 4. The adsorption sites of C_6H_6**@WYU-107** characterized by single-crystal X-ray diffraction.

As the pore sizes and functional ligands inserted in the host-framework have significant impact on the host-guest interactions, benzene vapor sorption isotherms at 298 K were measured, which showed typical type-I curves (Figure 2b) and verified significant interaction between the guest benzene and host-framework. Obviously, the saturated benzene adsorption capacities of **WYU-MOF** correlate with pore volumes, as well as the pore sizes, which the capacity order gradually decreases from mono-pyridyl to tri-pyridyl ligands insertion with the size of pyridyl ligand increases. Specifically, the uptakes of mono-pyridyl ligand modified **WYU-100** (10.83 mmol/g), **WYU-101** (11.37 mmol/g) and **WYU-102** (11.50 mmol/g) are lower than that of the parent **NU-1500(Fe)** (13.02 mmol/g), due to the reduction of pore volume after the insertion of mono-pyridyl ligands. Similarly, the uptakes of bi-pyridyl ligand modified **WYU-104** (10.50 mmol/g) and **WYU-105** (10.46 mmol/g) are higher than those of tri-pyridyl ligands modified **WYU-107** (10.07 mmol/g), **WYU-108** (9.47 mmol/g). It is worth noting that MOFs modified with ligands of amide groups, **WYU-103** (8.88 mmol/g) and **WYU-106** (7.99 mmol/g), exhibit poor benzene vapor uptakes, probably ascribed to that the charge density and distribution of ligand is not conducive to interact with benzene molecule. The saturation uptakes of **WYU-100~108** are not superior compared to those reported MOFs, [Zn_{12}(μ-O)$_3$(BTB)$_4$(MPTDC)$_9$] (NENU-513, H_3BTB = benzene-1,3,5-tribenzoic acid, H_2MPTDC = 3-methyl-4-phenylthieno[2,3-b]thiophene-2,5-dicarboxylic acid) (21.62 mmol/g), MIL-101(Cr) (15.84 mmol/g) and ZJU-520 (12.07 mmol/g) (Table S1).[13, 30-31]

Interestingly, further analysis shows that the frameworks modified with various pyridyl ligands exhibit exceptional benzene adsorption behaviors at relatively low pressures. Specifically, **WYU-100~108** exhibit significant steep increases at low pressures, indicating the great potential for the capture of benzene vapor at trace levels. According to the literature, the capture of benzene at low concentrations, especially at low-pressure (P/P_0 < 0.01) is critically important due to directly correlates with the challenging scenario of adsorbing highly diluted pollutants from air.[11, 32-34] This value corresponds to a partial benzene pressure of ~127 Pa, and equates to a benzene concentration of approximately 1250 ppm. Although the

View Article Online
DOI: 10.1039/D5SC05093F

concentration of benzene in polluted air or industrial settings present in parts-per-billion (ppb) and low parts-per-million (ppm) level, P/P_0 = 0.01 is usually used to simulate the trace conditions in the laboratory for investigating the capture performance of benzene.

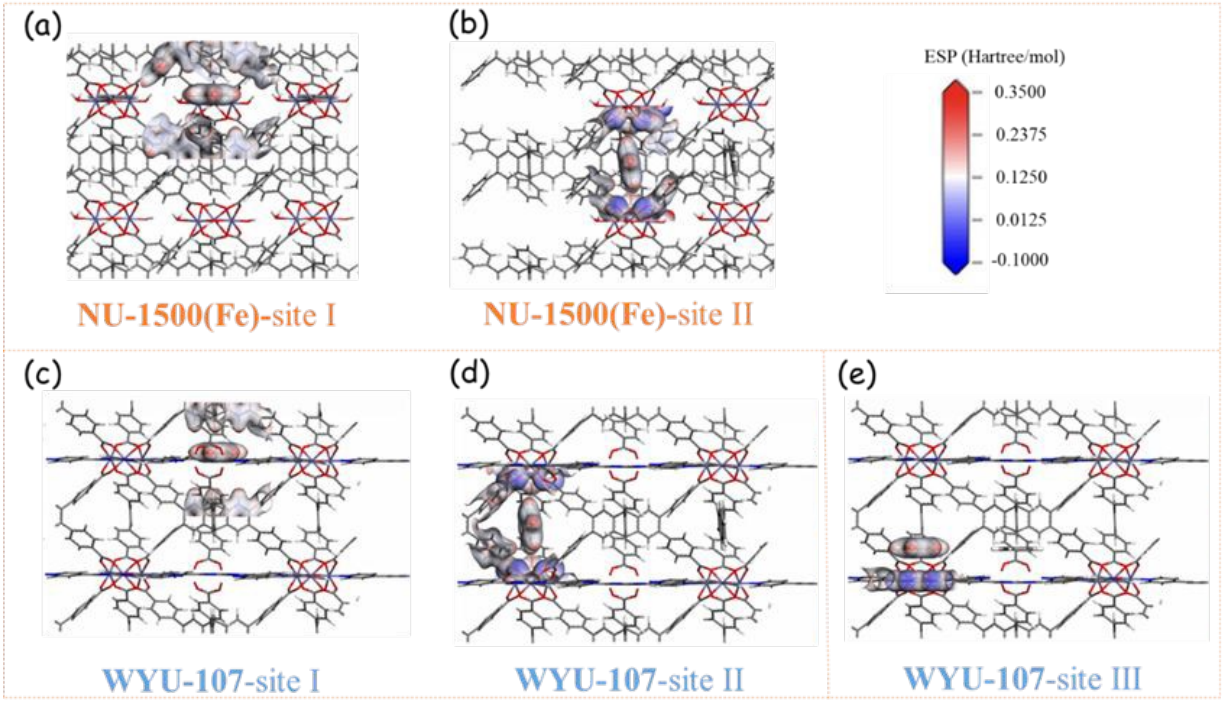

Figure 5. The ESP of adsorption binding sites in **NU-1500(Fe)** (a, b) and **WYU-107** (c-e).

For example, **WYU-100**, **WYU-101** and **WYU-102** show benzene uptakes of 3.93, 3.25 and 2.76 mmol/g at P/P_0 = 0.01, respectively, which are significantly higher than that (2.12 mmol/g) of their parent **NU-1500(Fe)**. At the same time, those of **WYU-103**, **WYU-104** and **WYU-105** are 5.59, 5.92 and 5.66 mmol/g, respectively, while those of **WYU-106**, **WYU-107** and **WYU-108** reach 3.23 mmol/g, 6.21 mmol/g and 5.20 mmol/g, respectively (Figure 2c). Notably, the uptake of **WYU-107** modified with tph ligand is about three times higher than that of **NU-1500(Fe)**. As far as we know, the trace adsorption capacity of **WYU-107** exceeds most porous materials, and is only under that of the defected-MIL-125-X (7.63 mmol/g, X = Mn, Co, Ni, Cu, Zn) (Figure 2d).[11, 13, 31, 33-35] In short, the pore volume is conducive to the satura-tion benzene uptakes, while the adsorption performance of trace benzene uptake is related to the sizes and struc-tures of the inserted ligands in the framework, which govern the host-guest interaction. Consequently, the uptakes of trace benzene vapor gradually increase from mono-pyridyl **WYU-100** to bi-pyridyl **WYU-105** to tri-pyridyl **WYU-107**. In addition, the benzene vapor uptake for **WYU-107** showed negligible diminishing after mul-tiple cycles, suggesting the significant reproducibility for **WYU-107** (Figure S24). In order to verify the structural distortions of the framework during the adsorption process, *in situ* variable-pressure PXRD of activated **WYU-107** were collected and show new diffraction peak (the highlighted zone) occurred with the pressure increase of benzene vapor. At the same time, the PXRD pattern of desorption at 120 °C was consistent with as-synthesized **WYU-107**, which may be attributed to deformation behaviour during the adsorption process (Figure 3a).

To evaluate the efficiency of **WYU-107** for the capture of trace benzene from different humidity (RH=0% and 40%), dynamic breakthrough experiments of **WYU-107** were performed. The results indicated benzene vapor started to breakthrough the column of ~3750 min/g under the dry conditions (RH= 0%), corresponding to a dynamic adsorption capacity of 6.64 mmol/g. However, the adsorption capacity reduced to 1.22 mmol/g (~652 min/g) under the humidity (RH= 40%) due to the competitive adsorption of water (Figures 3b and S25-S26). At the same time, adsorption kinetic experiments of benzene vapor were performed on **WYU-100**, **WYU-105** and **WYU-107** as examples at P/P_0 = 0.01. The results show that there are 12 minutes to reach adsorption equilibrium for **WYU-100**, while only 2 minutes for **WYU-107** with the macrocyclic ligands. Meanwhile, the adsorption uptake (5.90 mmol/g) of **WYU-107** is close to the value (6.21 mmol/g) from the adsorption isotherm at P/P_0 = 0.01. These results indicate that the PSM of macrocyclic ligands into **NU-1500(Fe)** can significantly enhance the host-guest interaction, which is conducive to the adsorption rate for benzene vapor (Figure S27).

To gain insight into the interaction mechanism between the framework of **WYU-107** and benzene molecules, **C_6H_6@WYU-107** was characterized by SCXRD, showing clearly the positions of benzene molecules in the pore (Figure 4). There are three binding sites (I, II and III) for C_6H_6 in **C_6H_6@WYU-107**. Specifically, sites I and II are located in the cavities enclosed by a pair of triptycence

View Article Online
DOI: 10.1039/D5SC06037F

moieties and a pair of trinuclear clusters, respectively. The benzene molecule in site I is bound to the triptycence moieties through C–H···π interactions (*d* = 3.7 to 4.4 Å), while that in site II is stabilized by C–H···π interactions (*d* = 4.2–4.5 Å), as well as strong C–H···O interactions with carboxylate groups (2.9-3.3 Å). Notably, a pair of benzene molecules are tightly encapsulated in site III enclosed by a pair of tph ligand, where each benzene molecule simultaneously interacts with the hexaazaphenalene moiety in a face-to-face
fashion at a short distance of *ca*. 3.4 Å and with the other benzene molecule at a distance of *ca*. 4.8 Å into special π-π stacking interactions.[40] Such strong host-guest interactions obviously contribute to the remarkable benzene uptake of **WYU-107** at low pressures compared to the parent **NU-1500(Fe)**, demonstrating the crucial role of macrocyclic tph in enhancing the binding interactions with benzene molecules. At the same time, the results of theoretical calculations for **C_6H_6@WYU-107** and **NU-1500(Fe)** demonstrate that the interaction sites are in substantial accordance with the *in situ* SCXRD.[41-43]

Furthermore, the calculations of electrostatic potential (ESP) indicated there are significant dispersion forces between benzene molecules and multiple adjacent atoms within host-framework at site I, due to the close distances. While strong induction and orientation forces occurred at site II due to the electrostatic interaction between hydrogen atoms (positive charge) of benzene and oxygen atoms (negative charge) of carboxylate groups. Specifically, the calculated binding energy of the benzene molecule in the parent **NU-1500(Fe)** at site II is −58.01 kJ/mol, which is slightly higher than that at site I of −57.23 kJ/mol (Figure 5a, 5b). In contrast, **WYU-107** possesses not only two adsorption sites (site I and II) similar to those of **NU-1500(Fe)**, with the calculated binding energies are −46.40 kJ/mol and −71.78 kJ/mol (Figure 5c, 5d), respectively, but also additional site III of calculated binding energy −33.71 kJ/mol (Figure 5e). In other words, the insertion of macrocyclic ligands induces structural deformation, resulting in the enhancement of host-guest interactions at site II, and introducing an extra site III in **WYU-107** at the same time. Consequently, such multiple effects result in the significantly enhance capture of trace benzene.

Conclusions

In summary, various pyridyl derivative ligands were successfully integrated into **NU-1500(Fe)** by post-synthetic modification strategy, allowing the regulation of host-guest interaction. Particularly, **WYU-107** modified with a tri-pyridyl ligand of functional macrocyclic moiety exhibits significant interaction for benzene molecules by virtue of the combination of π-π, C–H···π and C–H···O interactions, enabling the capture performance surpassing most reported porous materials. These results demonstrate that the enhancement of the host-guest interactions by post-synthetic modification of functional macrocyclic ligand insertion in large pores of MOFs is effective for the capture of trace benzene vapor, which may inspire the molecular design of porous materials to achieve higher capture efficiency.

Author Contributions

Gang Liang: investigation, data curation, writing - original draft. **De-Jian Chen:** methodology, data curation, resources. **Zhu-Jun Long:** methodology, data curation, resources. **Hao Zhou:** resources, methodology. **Xiao-Feng Zhong, Xiong-Hai Chen** and **Huai-Yu Shao:** ng - review & editing. **Zong-Wen Mo:** project administration, funding acquisition, writing - original draft, writing - review & editing, formal analysis. **Xiao-Ming Chen:** supervision, project administration, funding acquisition.

Conflicts of interest

The authors declare no competing financial interest

Acknowledgements

This work was supported by the Hong Kong–Macao Joint Research and Development Fund of Wuyi University (2022WGALH06), and NSFC (22090061). We also thank Ze Chang (Nankai University), Rui-Biao Lin and Wen-Bin Li (Sun Yat-Sen University) for their assistance with *in situ* PXRD and breakthrough test.

Notes and references

1 Y. Han, D. Brooks, M. He, Y. Chen, W. Huang, B. Tang, et al. Enhanced Benzene Adsorption in Chloro-Functionalized Metal-Organic Frameworks. *J. Am. Chem. Soc.* 146 (2024) 28080-28087.
2 T. N. Tu, T. M. Pham, Q. H. Nguyen, N. T. Tran, V. N. Le, L. H. Ngo, K. Chang&J. Kim Metal-organic frameworks for aromatic-based VOC capture. *Sep. Purif. Technol.* 333 (2024) 125883.
3 X. Li, L. Zhang, Z. Yang, P. Wang, Y. Yan&J. Ran Adsorption materials for volatile organic compounds (VOCs) and the key factors for VOCs adsorption process: A review. *Sep. Purif. Technol.* 235 (2020) 116213.

View Article Online
DOI: 10.1039/D5SC05093F

4 C. Lai, Z. Wang, L. Qin, Y. Fu, B. Li, M. Zhang, et al. Metal-organic frameworks as burgeoning materials for the capture and sensing of indoor VOCs and radon gases. *Coord. Chem. Rew.* 427 (2021) 213565.
5 R. C. Zhao, L. H. Xie, X. M. Liu, Z. Liu, X. Y. Li&J. R. Li Removal of Trace Benzene from Cyclohexane Using a MOF Molecular Sieve. *J. Am. Chem. Soc.* 147 (2024) 2467-2475.
6 L. Hu, M. Zhang, W. Wang, J. Hu, W. Wu, D. Lin&K. Yang A Novel Mesoporous Aluminum-Based MOF with Large Pore Volume for High Concentration Benzene Adsorption. *Advanced Functional Materials*. 35 (2025) 2425429.
7 O. I. F. Chen, C. H. Liu, K. Wang, E. Borrego Marin, H. Li, A. H. Alawadhi, J. A. R. Navarro&O. M. Yaghi Water-Enhanced Direct Air Capture of Carbon Dioxide in Metal-Organic Frameworks. *J. Am. Chem. Soc.* 146 (2024) 2835-2844.
8 D. Sengupta, S. Bose, X. Wang, N. M. Schweitzer, C. D. Malliakas, H. Xie, et al. Integrated CO_2 Capture and Conversion by a Robust Cu(I)-Based Metal–Organic Framework. *J. Am. Chem. Soc.* 146 (2024) 27006-27013.
9 H. Li, K. Wang, Y. Sun, C. T. Lollar, J. Li&H.-C. Zhou Recent advances in gas storage and separation using metal–organic frameworks. *Mater. Today*. 21 (2018) 108-121.
10 H. L. Zheng, J. Q. Zhao, Y. Y. Sun, A. A. Zhang, Y. J. Cheng, L. He, X. Bu, J. Zhang&Q. Lin Multilevel-Regulated Metal–Organic Framework Platform Integrating Pore Space Partition and Open-Metal Sites for Enhanced CO_2 Photoreduction to CO with Nearly 100% Selectivity. *J. Am. Chem. Soc.* 145 (2023) 27728-27739.
11 T. He, X. J. Kong, Z. X. Bian, Y. Z. Zhang, G. R. Si, L. H. Xie, et al. Trace removal of benzene vapour using double-walled metal–dipyrazolate frameworks. *Nat. Mater.* 21 (2022) 689-695.
12 C. Gu, N. Hosono, J. J. Zheng, Y. Sato, S. Kusaka, S. Sakaki&S. Kitagawa Design and control of gas diffusion process in a nanoporous soft crystal. *Science*. 363 (2019) 387-391.
13 L. Hu, W. Wu, M. Hu, L. Jiang, D. Lin, J. Wu&K. Yang Double-walled Al-based MOF with large microporous specific surface area for trace benzene adsorption. *Nat. Commun.* 15 (2024) 3204.
14 Y. Han, W. Huang, M. He, B. An, Y. Chen, X. Han, et al. Trace benzene capture by decoration of structural defects in metal–organic framework materials. *Nat. Mater.* 23 (2024) 1531-1538.
15 Z. H. Qiu, J. H. Li, B. X. He, P. Q. Liao, M. Y. Zhou, P. X. Li, R. B. Lin, J. P. Zhang&X. M. Chen Fast adsorption and kinetic separation of benzene and cyclohexane/cyclohexene in a microporous metal azolate framework. *J. Mater. Chem. A*. 12 (2024) 13240-13246.
16 X. Zhao, Y. Wang, D. S. Li, X. Bu&P. Feng Metal–Organic Frameworks for Separation. *Adv. Mater.* 30 (2018) 1705189.
17 W. B. Li, Y. Wu, X. F. Zhong, X. H. Chen, G. Liang, J. W. Ye, Z. W. Mo&X. M. Chen Fluorescence Enhancement of a Metal-Organic Framework for Ultra-Efficient Detection of Trace Benzene Vapor. *Angew. Chem., Int. Ed.* 62 (2023) e202303500.
18 C. X. Chen, Z. W. Wei, J. J. Jiang, S. P. Zheng, H. P. Wang, Q. F. Qiu, C. C. Cao, D. Fenske&C. Y. Su Dynamic Spacer Installation for Multirole Metal–Organic Frameworks: A New Direction toward Multifunctional MOFs Achieving Ultrahigh Methane Storage Working Capacity. *J. Am. Chem. Soc.* 139 (2017) 6034-6037.
19 Y. Hu, X. Zhang, R. S. H. Khoo, C. Fiankor, X. Zhang&J. Zhang Stepwise Assembly of Quinary Multivariate Metal-Organic Frameworks via Diversified Linker Exchange and Installation. *J. Am. Chem. Soc.* 145 (2023) 13929-13937.
20 O. I. F. Chen, C. H. Liu, K. Wang, E. Borrego Marin, H. Li, A. H. Alawadhi, J. A. R. Navarro&O. M. Yaghi Water-Enhanced Direct Air Capture of Carbon Dioxide in Metal–Organic Frameworks. *J. Am. Chem. Soc.* 146 (2024) 2835-2844.
21 B. Li, D. Ma, Y. Li, Y. Zhang, G. Li, Z. Shi, S. Feng, M. J. Zaworotko&S. Ma Dual Functionalized Cages in Metal–Organic Frameworks via Stepwise Postsynthetic Modification. *Chem. Mater*. 28 (2016) 4781-4786.
22 Z. Chen, P. Li, X. Zhang, P. Li, M. C. Wasson, T. Islamoglu, J. F. Stoddart&O. K. Farha Reticular Access to Highly Porous acs-MOFs with Rigid Trigonal Prismatic Linkers for Water Sorption. *J. Am. Chem. Soc.* 141 (2019) 2900-2905.
23 S.-S. Meng, M. Xu, H. Guan, C. Chen, P. Cai, B. Dong, et al. Anisotropic flexibility and rigidification in a TPE-based Zr-MOFs with scu topology. *Nat. Commun.* 14 (2023) 5347.
24 M. J. Hurlock, L. Hao, K. W. Kriegsman, X. Guo, M. O'Keeffe&Q. Zhang Evolution of 14-Connected Zr_6 Secondary Building Units through Postsynthetic Linker Incorporation. *ACS Appl. Mater. Interfaces*. 13 (2021) 51945-51953.
25 A. N. Hong, E. Kusumoputro, Y. Wang, H. Yang, Y. Chen, X. Bu&P. Feng Simultaneous Control of Pore-Space Partition and Charge Distribution in Multi-Modular Metal–Organic Frameworks. *Angew. Chem., Int. Ed.* 61 (2022) e202116064.
26 M. Kang, D. W. Kang&C. S. Hong Post-synthetic diamine-functionalization of MOF-74 type frameworks for effective carbon dioxide separation. *Dalton Trans.* 48 (2019) 2263-2270.
27 P. Horcajada, F. Salles, S. Wuttke, T. Devic, D. Heurtaux, G. Maurin, et al. How Linker's Modification Controls Swelling Properties of Highly Flexible Iron(III) Dicarboxylates MIL-88. *J. Am. Chem. Soc.* 133 (2011) 17839-17847.
28 Y. Chen, H. Xie, Y. Zhong, F. Sha, K. O. Kirlikovali, X. Wang, C. Zhang, Z. Li&O. K. Farha Programmable Water Sorption through Linker Installation into a Zirconium Metal-Organic Framework. *J. Am. Chem. Soc.* 146 (2024) 11202-11210.
29 Z. S. Wang, X. W. Zhang, K. Zheng, X. X. Chen, D. D. Zhou&J. P. Zhang A topology approach to overcome the pore size/volume trade-offs for autonomous indoor humidity control. *Sci. China Chem.* 67 (2024) 2968-2974.
30 W. W. He, G. S. Yang, Y. J. Tang, S. L. Li, S. R. Zhang, Z. M. Su&Y. Q. Lan Phenyl Groups Result in the Highest Benzene Storage and Most Efficient Desulfurization in a Series of Isostructural Metal-Organic Frameworks. *Chem. Eur. J.* 21 (2015) 9784-9789.
31 L. H. Xie, X. M. Liu, T. He&J. R. Li Metal-Organic Frameworks for the Capture of Trace Aromatic Volatile Organic Compounds. *Chem*. 4 (2018) 1911-1927.
32 J. Yuan, X. Liu, M. Li&H. Wang Design of nanoporous materials for trace removal of benzene through high throughput screening. *Sep. Purif. Technol.* 324 (2023) 124558.
33 Y. Han, Y. Chen, Y. Ma, J. Bailey, Z. Wang, D. Lee, et al. Control of the pore chemistry in metal-organic frameworks for efficient adsorption of benzene and separation of benzene/cyclohexane. *Chem*. 9 (2023) 739-754.
34 L. Hu, W. Wang, X. Miao, M. Hu, D. Luo, W. Wu, D. Lin&K. Yang A novel Al-based MOF with straight channel and pocket pore structure for trace benzene adsorption and benzene/cyclohexane separation. *Chem. Eng. J.* 499 (2024) 156376.
35 L. Hu, W. Wu, L. Gong, H. Zhu, L. Jiang, M. Hu, D. Lin&K. Yang A Novel Aluminum-Based Metal-Organic Framework with Uniform Micropores for Trace BTEX Adsorption. *Angew. Chem., Int. Ed.* 62 (2023) e202215296.
36 Y. Z. Zhang, X. D. Zhang, Y. K. Zhang, F. T. Wang, L. l. Geng, H. Hu, et al. Linker engineering in mixed-ligand metal-organic frameworks for simultaneously enhanced benzene adsorption and benzene/cyclohexane separation. *Inorg. Chem. Front.* 11 (2024) 8101-8109.

View Article Online
DOI: 10.1039/D5SC05093F

37 Z. Chen, P. Fang, J. Li, X. Han, W. Huang, W. Cui, et al. Rapid extraction of trace benzene by a crown-ether-based metal-organic framework. *Natl. Sci. Rev.* 11 (2024) nwae342.
38 L. K. Macreadie, E. J. Mensforth, R. Babarao, K. Konstas, S. G. Telfer, C. M. Doherty, J. Tsanaktsidis, S. R. Batten&M. R. Hill CUB-5: A Contoured Aliphatic Pore Environment in a Cubic Framework with Potential for Benzene Separation Applications. *J. Am. Chem. Soc.* 141 (2019) 3828-3832.
39 J. Chang, F. Chen, H. Li, J. Suo, H. Zheng, J. Zhang, et al. Three-dimensional covalent organic frameworks with nia nets for efficient separation of benzene/cyclohexane mixtures. *Nat. Commun.* 15 (2024) 813.
40 C. X. Ren, L. X. Cai, C. Chen, B. Tan, Y. J. Zhang&J. Zhang π-Conjugation-directed highly selective adsorption of benzene over cyclohexane. *J. Mater. Chem. A*. 2 (2014) 9015-9019.
41 S. Grimme, J. Antony, S. Ehrlich&H. Krieg A consistent and accurate ab initio parametrization of density functional dispersion correction (DFT-D) for the 94 elements H-Pu. *J. Chem. Phys.* 132 (2010) 154104.
42 T. D. Kühne, M. Iannuzzi, M. Del Ben, V. V. Rybkin, P. Seewald, F. Stein, et al. CP2K: An electronic structure and molecular dynamics software package-Quickstep: Efficient and accurate electronic structure calculations. *J. Chem. Phys.* 152 (2020) 194103.
43 J. VandeVondele&J. Hutter An efficient orbital transformation method for electronic structure calculations. *J. Chem. Phys.* 118 (2003) 4365-4369.

View Article Online
DOI: 10.1039/D5SC05093F

Data availability

The data that support the findings of this study are available from the corresponding author upon reasonable request.